INTERNATIONAL JOURNAL OF LATEST TECHNOLOGY IN ENGINEERING, MANAGEMENT & APPLIED SCIENCE (IJLTEMAS)

ISSN 2278-2540 | DOI: 10.51583/IJLTEMAS | Volume XII, Issue IX, September 2023

Effects of Reservoir Angle on Vertical Well Performance

[1]Maurice Akpan Blessing, [2]Osisanya Olajuwon Wasiu, [3]Ogugu Augustine Abiodun, [4]Onyekwere Kelechi Raymond

[1]Department of Petroleum Engineering, Federal University of Petroleum Resources, Effurun, Delta State, Nigeria

[2]Department of Physics, Faculty of Physical Science, University of Benin, Edo State, Nigeria

[3,4]Department of Petroleum Engineering and Geosciences, Petroleum Training Institute, Effurun, Nigeria.

DOI: https://doi.org/10.51583/IJLTEMAS.2023.12905

Received: 08 July 2023; Revised: 06 September 2023; Accepted: 12 September 2023; Published: 29 September 2023

Abstract: Petroleum engineers are desperately needed to maintain sustained clean oil production for a long time without running into flow restrictions caused by external boundaries. These boundaries could take the shape of sealing faults, which are the most frequent in real-world situations, constant-pressure boundaries, or other reservoir heterogeneities, such as fractures, layers, and lateral discontinuities, to name a few. This study aims to examine the impact of reservoir angle on the efficiency of vertical oil wells. In this study, empirical mathematical models were used to describe vertical oil wells constrained by two sealing faults in a reservoir supported by a strong aquifer. The mathematical models developed by (1) are applied by computer software. It was determined after evaluation that lower reservoir angles provide greater values of pressure derivatives, which is indicative of good productivity and performance. To evaluate the impact of the reservoir angle on dimensionless pressure and pressure derivatives, a sensitivity analysis was also conducted utilizing a fixed value of dimensionless time to study various reservoir angle values. However, it was shown that the dimensionless pressure, PD, is unaffected by the reservoir angle. The dimensionless pressure derivative (P'D) was shown to have an inverse relationship with the reservoir angles. To verify the accuracy of the results, a comparison analysis between the findings from the constructed computer model, OBLIQ, and those found in the literature was carried out. The analysis' findings demonstrated that the study's finding is consistent with those in the literature.

Keywords: Model, reservoir, flow, angle, well

I. Introduction

Following the discovery of crude oil, it is typically crucial to characterize the reservoir for key factors such as reservoir extent (area), porosity, permeability, and fluid saturation. To optimize future production and ultimately recover economically viable hydrocarbons, a thorough examination through coring, well tests, etc. must be conducted to better define the behavior of the subterranean deposit (2) applied the theory of images for the first time to multiple boundary reservoirs. The analysis of the pressure transient in the presence of two intersecting boundaries was presented by (3). The angle between the boundaries, flow capacity, proximity to the fault, and initial reservoir pressure were all calculated using the least squares approach. According to earlier research, sealing flaws cause a difference between a well's pressure response and a homogenous line source's response. According to (4), "the size, shape, and orientation of the impermeable region are highly correlated with the pressure response." A vertical well is located at the center of the circular reservoir. Its wellbore radius is round bottom-hole pressure is pwf. the average reservoir pressure, the kind and size of the reservoir border, heterogeneity, fluid properties, and wellbore characteristics are just a few examples of reservoir metrics that help reservoir specialist make important management decisions (5). Type curves have been used for a reservoir's correct description and characterization over the years. Following that, the dimensionless parameters defining that type curve can be used to compute the reservoir and well parameters (such as permeability and skin). Two steps make up the interpretation of well test results: establishing the well/reservoir system and calculating the system's governing parameters. The difficulties associated with employing straight-line approaches have been largely overcome by the use of dimensionless pressure and dimensionless pressure derivative-type curves, leading to notable accomplishments in the analysis of well tests. Information like pressure distribution is crucial in defining wellbore pressure regimes and acceptable rate profiles when a reservoir is restricted by persistent bottom water to ensure clean oil production. Using data from a well situated between a constant pressure barrier and a sealing fault, (6) conducted a study to describe the behavior of the well. In their type curves produced to assess dimensionless pressure drop, three distinct slopes could be seen. The notion of picture wells was demonstrated in the paper along with superposition in time to allow for test periods with various flow rates. The angles taken into account are 30, 45, 90, and 120 degrees. It was shown that decreasing angles increase both pressure change and derivative. Engineers can determine the reservoir's long-term performance by locating these faults and accurately estimating how far away or where a well should be located from a fault to avoid interference. However, the focus of the study conducted by (7) was on pinpointing the best well location using magnitudes

ISSN 2278-2540 | DOI: 10.51583/IJLTEMAS | Volume XII, Issue IX, September 2023

of dimensionless pressure derivatives for various separations of a production well from inclined reservoir boundaries. Considered to be sealing and sloping were the external limits. They looked at the behavior of a well's pressure and pressure derivative behavior close to two intersecting leaky faults that formed angles of 120°, 90°, 60°, and 45°, respectively. According to (7), reservoir characterization serves as the foundation for all reservoir engineering analyses, from straightforward analytical evaluations to more complex reservoir simulation assignments. Additionally, they confirmed that the industry uses pressure transient analysis effectively to identify the different types of reservoir boundaries. These boundaries may be "sealing" or "non-sealing" in nature. Similarly, Petroleum engineers are essential to sustaining sustained clean oil production without running into flow constraints caused by external boundaries. These barriers could take the shape of constant-pressure boundaries, sealing faults (which are most frequently encountered in practice), or other reservoir heterogeneities, such as fractures, layers, and lateral discontinuities, to name a few. When any of these heterogeneities are present in a formation, it is extremely difficult to analyze how the reservoir system responds to pressure (8).

This study intends to look into how vertical well performance is affected by reservoir angle. However, the following list of study goals is provided:

1. To apply vertical flow models for reservoirs with sealing faults in order to explore how reservoir angle affects the performance of vertical wells.
2. Creating a computer program to calculate dimensionless pressure derivatives at various reservoir angles.
3. Display charts of dimensionless pressures against dimensionless time at various reservoir angles to assess the effectiveness of vertical wells.
4. To confirm findings by contrasting them with findings from the literature.

II. Related Literature

(9) presented the first work on the detection of a linear fluid barrier/fault from pressure transient data. The foundation for the pressure transient study of a single well located near a sealing fault was also presented. Horner estimated the approximate distance from a fault using pressure build-up data. This was achieved by applying the method of images. As a result of this initial study, there was a breakthrough in the investigation and identification of hydrocarbon reservoirs using pressure transient testing. The pressure transient curves must have certain features to produce valid data. These features were identified by (10) Using pressure drawdown data, they also presented an equation for calculating the relative distance to a fault. The first application of the theory of images to multiple boundary reservoirs was carried out by (2). (11) presented the analysis of pressure transient in the presence of two intersecting boundaries. The following reservoir parameters were determined using the least squares method: angle between the boundaries, flow capacity, relative distance to the fault, and the initial reservoir pressure. From previous studies, it is seen that sealing faults result in a deviation between the pressure response of a well and the response of a homogeneous line source. (4) "determined that pressure response is extremely sensitive to the size, shape, and orientation of the impermeable region". (6) carried out a study aimed at characterizing the behavior of a well located between a constant pressure boundary and a sealing fault. Three distinct slopes were visible in their results of type curves generated to evaluate dimensionless pressure drop. The first slope signified flow in an infinite reservoir; the second slope identified the presence of the no-flow or sealing boundary; and the third slope corresponded to the presence of a constant pressure boundary. Furthermore, the study showed that the production well displayed transient flow behavior for a longer period as the distance between the two boundaries increased. After the real/object well senses a boundary, it starts deviating from the initial straight line and a second slope is formed indicating the presence of a no-flow boundary. This second slope is a direct function of the well's distance from the no-flow boundary. The detection of this no-flow boundary restricts the reservoir extent on one side of the well's production zone while the production rate has remained constant, they added. (12), presented the effect of sealing wedge angle on well test behavior. The paper illustrated the concept of image wells in conjunction with superposition in time to account for test periods with different flow rates. The angles considered include 30°, 45°, 90°, and 120°. It was observed that both pressure change and derivative increase with decreasing angles. (7) propounded that reservoir characterization forms the basis of all reservoir engineering analysis, from conventional evaluations done analytically to more involved reservoir simulation tasks. They also affirmed that the use of pressure transient analysis in the industry is efficient in determining reservoir boundary types. The nature of these boundaries can either be "sealing" or "non-sealing". The identification of these faults as well as accurate estimation of the optimum distance or location of an active well from a fault enables engineers to ascertain the long- term performance of the reservoir. Nevertheless, the study performed by (7) was centered on determining the optimum well location using magnitudes of dimensionless pressure derivatives for different distances of a production well from inclined reservoir boundaries using the dimensionless pressure derivative expression for vertical wells. The external boundaries were considered to be sealing and inclined. They studied the pressure and pressure derivative behavior of a well near two intersecting leaky faults forming an angle of 120°, 90°, 60°, and 45° respectively. The derivatives were computed from the total dimensionless pressure expression summing all the image wells by the superposition principle. Moreover, results obtained from the study of (7)

ISSN 2278-2540 | DOI: 10.51583/IJLTEMAS | Volume XII, Issue IX, September 2023

revealed that the optimum well location from the sealing faults is inversely proportional to the inclined angles. This implies that wells closer to faults produce optimally at any given time. Furthermore, the relationship between good distance and productivity has no maximum or minimum points. Other conclusions made from their research include;

i. The optimum well location for sealing boundaries depends on many factors, such as production profile, well design, faults angle, fluid type, and lease size.
ii. The wellbore radius has no significant effect on the dimensionless pressure derivative, optimum well location, and optimum time of production.

Influence of faults on reservoir performance

Fig. 1, show the faults are in partial communication with the other portions of the same formation on both sides. In the case of petroleum rocks, this type of partial communication causes additional pressure drop/support to the middle reservoir along with the producing wells. According to (13), wherever a fault occurs in the subsurface, it creates a fault zone and there is mechanical mixing of rock within this zone. On a seismic scale, most faults are interpreted as lines representing discontinuities in the subsurface, however in reality these are more complex. On outcrops, it can be observed that fault zones are heterogeneous and have some thickness (width), which can include cataclastic zones and shale smears, as shown in Fig. 2. Rock properties in fault zones can be redistributed and reconfigured typically causing a reduction of permeability across the fault zone width. The existence, location, and geometry of faults have a large impact on reservoir volumes, reservoir connectivity, and compartmentalization. Understanding these uncertainties is important in well planning or if one wants to perform history matching. An uncertainty model for the fault geometry makes it possible to run Monte Carlo simulation of the fault surfaces. This lets us analyze the uncertainty of the reservoir volumes, the probability *(for different compartmentalization scenarios, or analyze uncertainty in reservoir communication and reservoir flow (14*). Generally, fault permeability and thickness (width) control how faults behave during production. During production the drawdown by a producing well in a fault block can exert some pressure on the fault zone; however, 'catastrophic' fault breakdown as a result of this exerted pressure is not easily observed.

Modeling of fault zones along petroleum reservoirs

The influence of partially communicating fault on interference testing was first considered by (15), who introduced the idea of modeling the fault zone as a linear, vertical semi- permeable barrier of negligible capacity. Of course, the model is a great simplification of the complex physical nature of the zone, but as (15) noted, it has the essential property of imposing a linear flow pattern at the fault plane. It is also how partially communicating faults are modeled in reservoir simulation studies. (15) developed was obtained by numerical simulation. In essence, a partially communicating fault is a type of linear discontinuity in reservoir properties. Although the subject of linear discontinuities has often been addressed in the [transient well-testing literature, it has usually been concerned with scaling faults. (16) however, considered a case of an abrupt, linear change in the reservoir or fluid properties, as shown in Fig. 2.3a.

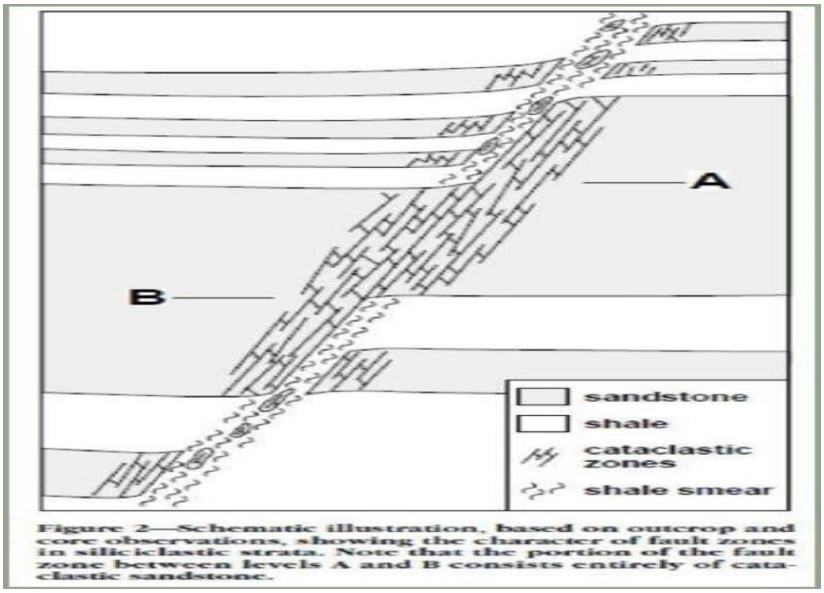

Figure 2—Schematic illustration, based on outcrop and core observations, showing the character of fault zones in siliciclastic strata. Note that the portion of the fault zone between levels A and B consists entirely of cataclastic sandstone.

Fig. 1**:** Schematic showing the character of fault zones (Gibson, 1994)

ISSN 2278-2540 | DOI: 10.51583/IJLTEMAS | Volume XII, Issue IX, September 2023

For comparison, the vertical semi-permeable barrier as shown in Fig. 2, the two problems look similar, but the mathematical models needed to describe them are quite different. Nevertheless, the solution technique (16) used can be used to solve the problem of a vertical semi-permeable barrier.

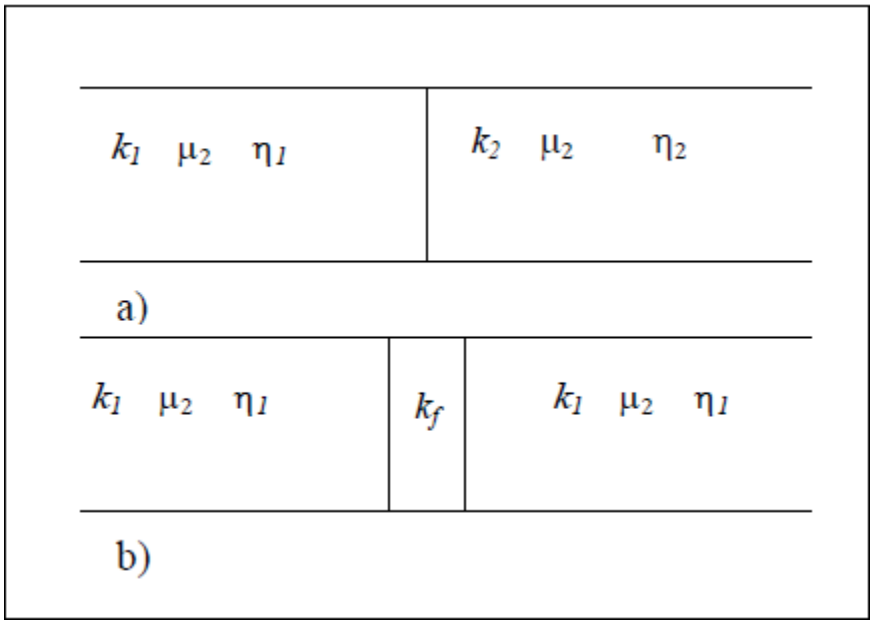

Fig. 2: Type of linear discontinuities: (a) abrupt change of rock and fluid properties; (b) vertical semipermeable barrier (17).

Yaxley Analytical solution

The problem under consideration for this model is the drawdown distribution resulting from constant rate production from a well in an infinite reservoir containing a linear, vertical semi-permeable barrier. The mathematical model relies on the assumptions that:

i. The reservoir fluid is single-phase and slightly compressible, with constant viscosity and compressibility.
ii. The reservoir is homogenous in all rock properties and isotropic with respect to permeability on each side of the semipermeable barrier.
iii. The formation thickness is constant.
iv. An infinite line source can be used to approximate the well.
v. The semi-permeable barrier is infinitely long and has negligible capacity.
vi. The fluid leakage rate through the semipermeable barrier is always proportional to the instantaneous pressure difference across the barrier.

The last two assumptions allow the partially communicating fault to be approximated by a vertical plane. This ought to be true if the fault zone's width is small in comparison to the distance between the fault plane and the well. (15) characterized the partially communicating fault by the parameter ratio kf/lf, which was defined as the fault conductivity. On both sides of the fault, the pressure behavior obeys the diffusivity equation, which is usually expressed in radial coordinates for problems of fluid flow to a well in a porous medium. The problem considered for (18) model, however, is more easily solved by expression of the diffusivity equation in Cartesian coordinates with a separate formulation for each side of the semi-permeable barrier. Nevertheless, (18) has obtained the solution to the pressure distribution as shown in equations 1 to 2;

$$P_D(xD, yD) = \frac{1}{2} Ei\left\{\frac{[(x-1)^2+y_D^2]}{4t_{DL}}\right\} - \frac{1}{2} Ei\left\{\frac{[(x-1)^2+y_D^2]}{4t_{DL}}\right\} - \sqrt{\pi} \propto_L \exp[2 \propto_L (x_D + 1)]$$

$$\times \int_0^{t_{DA}} \left\{\exp\left(4 \propto_A^2 u - \frac{y_D^2}{4u}\right) erfc\left[2 \propto_A \sqrt{u} + \frac{x_D + 1}{2\sqrt{u}}\right] \frac{du}{\sqrt{u}}\right\} - - - - \quad (1)$$

Where $t_{DA} = \delta t / b^2$ and

ISSN 2278-2540 | DOI: 10.51583/IJLTEMAS | Volume XII, Issue IX, September 2023

$$\propto_A = \frac{\left(\frac{k_f}{l_f \mu}\right)}{\frac{kh}{b\mu}}$$

The new dimensionless parameter, α_A is defined as the specific transmissibility ratio with respect to the fault distance *b.* Drawdown at the active well is obtained by setting $x=b-r_w$. and y = 0. If the wellbore radius (r_w) is very small as compared with the fault distance, *b,* then $xD+1=2$ and the wellbore pressure response is given by:

$$P_D(xD, yD) = \frac{1}{2} Ei\left\{\frac{r_{DW}^2}{4t_D L}\right\} - \frac{1}{2} Ei\left\{\frac{1}{4t_D L}\right\}$$

$$-\sqrt{\pi} \propto_A \times \int_0^{t_{DA}} \left\{\exp(4 \propto_A^2 u + 4 \propto_A) erfc\left[2 \propto_A \sqrt{u} + \frac{1}{\sqrt{u}}\right]\frac{du}{\sqrt{u}}\right\} - - - (2)$$

Where $r_{Dw}=rw/b$. This Equation contains, like its first two terms, the well-known method of images, a solution for a sealing fault and degenerates to the solution of homogeneous reservoirs when $\alpha_A = 0$ (17).

It was discovered that using this mathematical model causes some difficulties in calculations due to the very complex equations used in this model, particularly the term that contains an in tegral of the "erfc" function multiplied by an exponential function, which made thecal culation very difficult and led to the evaluation of some terms numerically.

Well flow models

In (19), proposed two basic well flow models in their paper. These flow models are outlined as follows;

i. Horizontal well flow models and
ii. Vertical flow models.

However, they considered two flow periods (early radial and final flow) while comparing the pressure distribution between horizontal and vertical wells. The well geometry for both horizontal and vertical well flow models is presentedin Fig.3 and Fig. 4 respectively. Fig. 3 depicts a horizontal well completion while Fig. 5 represents a vertical well completion. (19) assumed that both conditions are subjected to edge water drive also containing oil of small and constant compressibility. (20) give the approximate period of radial flow in vertical wells as $10^{-6} \leq t_{De} \leq 0.25 reD^2$. This implies that after time $t_{De} \geq 0.25$ reD2, the radial flow ends and the reservoir external boundary effects.

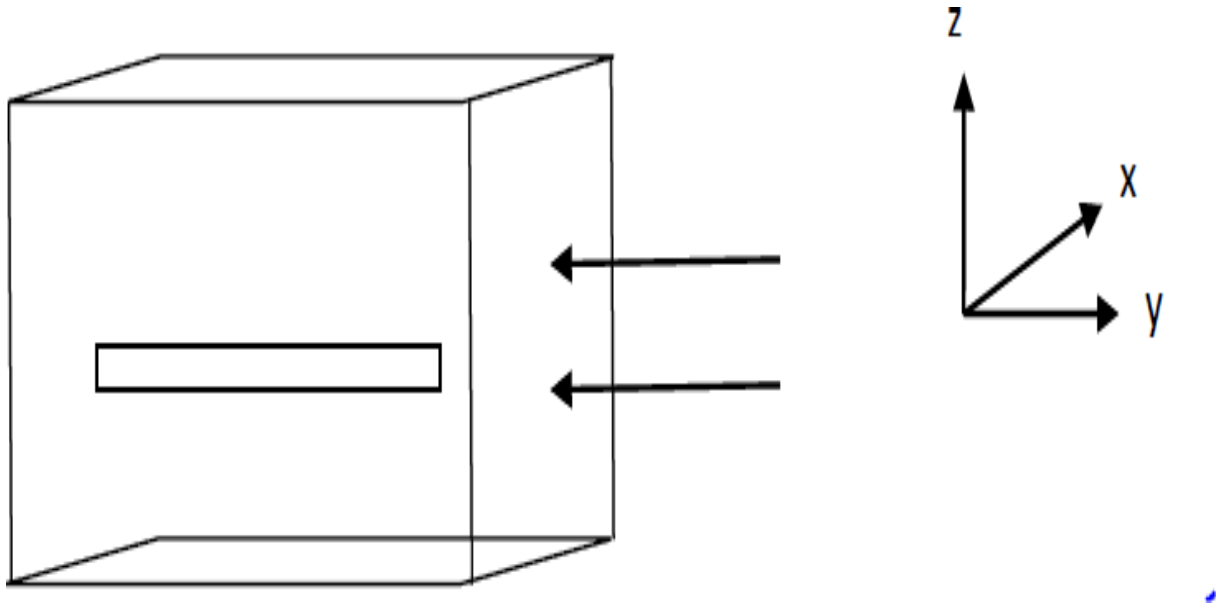

Fig. 3**:** Horizontal well model in a reservoir subject to water edge drive (19)

ISSN 2278-2540 | DOI: 10.51583/IJLTEMAS | Volume XII, Issue IX, September 2023

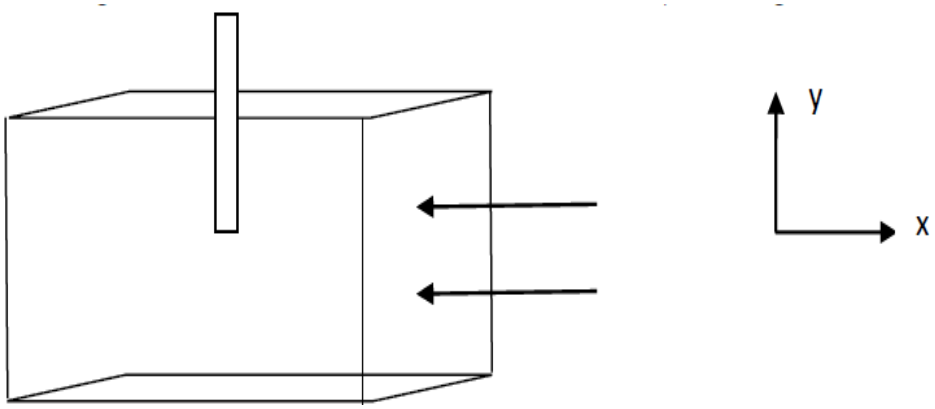

Fig. 4: Horizontal well model in a reservoir subject to water edge drive (19)

Horizontal flow models

Along the x–axis, according to (21) the source is an infinite plane source in an infinite slab source. The mathematical expression for this well model is shown in equations 3 to 5 respectively;

$$s(x_D, t_D) = \frac{2}{x_{eD}} \sum_{n=1}^{\infty} exp\left(-\frac{(2n+1)^2\pi^2 t_D}{4x_{eD}^2}\right) cos\frac{(2n+1)n\pi x_D}{x_{eD}} \cos(2n+1)\pi - - - (3)$$

Also, along the y-axis,

$$s(y_D, t_D) = \frac{1}{y_{eD}}\left[1 + 2\sum_{n=1}^{\infty} exp\left(\frac{-n^2\pi^2 t_D}{y_{eD}^2}\right) cos\frac{n\pi y_{wD}}{y_{eD}} \cos\frac{n\pi y_D}{y_{eD}}\right] - - - (4)$$

Along the z-axis, the well experiences driving forces from both the top and bottom ends, both capable of fomenting a steady-state. Therefore, the source is an infinite slab source in an infinite plane reservoir (22).

The z-axis is illustrated mathematically equation 5;

$$s(z_D, t_D) = \frac{1}{h_D}\left[1 + 2\sum_{n=1}^{\infty} exp\left(\frac{-l^2\pi^2 t_D}{h_D^2}\right) cos\frac{l\pi z_{wD}}{h_D} \cos\frac{l\pi z_D}{h_D}\right] - - - - - (5)$$

Where r_D = dimensionless radius h_D= dimensionless height

x_D= arbitrary dimensionless distance along the x-axis

y_D= arbitrary dimensionless distance along the y-axis

z_D= arbitrary dimensionless distance along the z-axis

L= Horizontal well length, ft

Z_{wD}= dimensionless well stand-off.

In recent works of literatures, (22) considered the flow of a slightly compressible fluid to a horizontal well of dimensionless length, L_D, in a reservoir of dimensionless thickness, h_D.in their research, the following assumptions were made;

i. The well is parallel to the top and bottom boundaries of a box-shaped drainage region.
ii. The well is located at an elevation, of Z_wD=0.5hD, from the bottom boundary.
iii. The well is a line source with the top and bottom boundaries permeable.
iv. The right edge of the reservoir is also permeable.
v. The reservoir pressure is above bubble point pressure and the production energy of the reservoir is the expanding gas cap and the aquifer support and not the dissolved gas.

However, wellbore storage and skin effects were not taken into account. The model description (i.e. the reservoir and wellbore configuration.) is illustrated in Fig. 5.

ISSN 2278-2540 | DOI: 10.51583/IJLTEMAS | Volume XII, Issue IX, September 2023

i. The well is a line source with the top and bottom boundaries permeable.
ii. The right edge of the reservoir is also permeable.
iii. The reservoir pressure is above bubble point pressure and the production energy of the reservoir is the expanding gas cap and the aquifer support and not the dissolved gas.

However, wellbore storage and skin effects were not taken into account. The model description (i.e. the reservoir and wellbore configuration.) is illustrated in Fig. 5.

Vertical flow models

Since the reservoir is experiencing edge water along the x-axis in this type of flow model, the system is always being recharged. According to (19), the reservoir is an infinite slab with an infinite planar source as the source. Anendless slab source. An illustration of the mathematical expression for this well model is presented in equations 6 to 7;

$$s(x_D, t_D) = \frac{2}{xe}\sum_{n=1}^{\infty} exp\left(-\frac{(2n+1)^2\pi^2 t_D}{4Xe^2}\right) cos\frac{(2n+1)n\pi X}{Xe} \cos(2n+1)\pi --- (6)$$

Also, along the y-axis,

$$s(y_D, t_D) = \frac{1}{ye}\left[1 + 2\sum_{n=1}^{\infty} exp\left(\frac{-n^2\pi^2 t_D}{y^2}\right) sin\frac{n\pi yw}{ye} \sin\frac{n\pi y}{ye}\right] --- (7)$$

The pressure distribution for a two-layered reservoir was calculated in a work by (23). Figure 5 depicts the arrangement of the described reservoir. The two-layered reservoir in their analysis was believed to contain oil with a small and constant compressibility in each layer. As shown in Fig. 7, the layers are penetrated by a vertical well, and depending on the fluid dynamics and interlayer degree of crossflow, either one layer in particular or both layers may be finished for production. A constant pressure gas cap is placed on top of the reservoir, and bottom water is present at the bottom. (23) explored the effects of layering in vertical well flow models under the following presumptions:

f = 0.5, x_D = 4.0, z_D = 0.7, M = 0.9, and = 10 are the values. The aforementioned facts imply that oil production from the two levels occurs where the vertical well is finished in Layer 1. The values of = 10 and M = 0.9 indicate that for layers containing oil of the same viscosity and thickness, Layer 2's permeability is greater than Layer 1's, and the interface's degree of crossflow is 10. Greater crossflow would result in greater interface permeability. Interlayer flow would experience a significant delay due to a contact with low permeability.

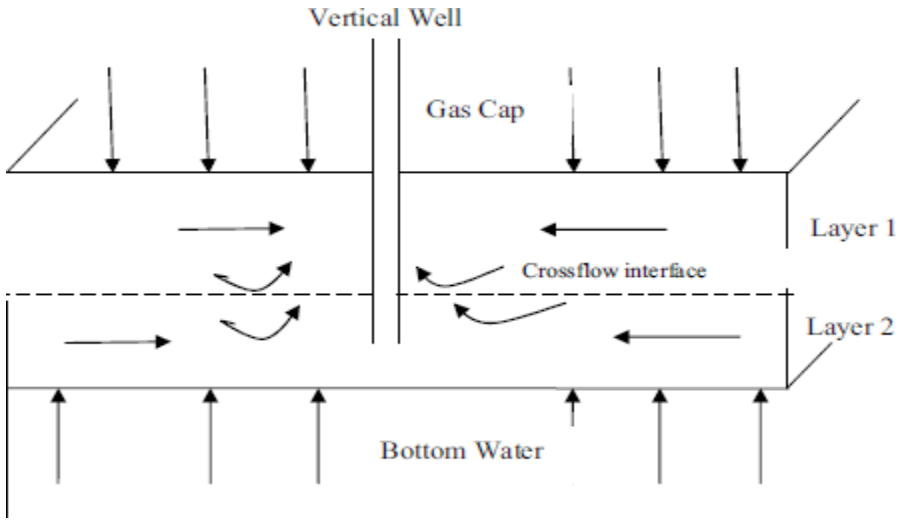

Fig. 5: Vertical reservoir well model description (23)

Layering is the primary reason for gradient variations, especially at late flow dimensionless periods, as demonstrated on a log-log plot of dimensionless pressure vs dimensionless time in Fig. 5. According to the various gradients, the contribution of each layer to flow is inversely correlated with their regional permeability. In the derivative plot, it appears as a depression whereas it appears as a gradual climb in the pressure plot. A depression on the derivative plot indicates the meeting with a constant-pressure boundary,

ISSN 2278-2540 | DOI: 10.51583/IJLTEMAS | Volume XII, Issue IX, September 2023

and a rise following a depression indicates the contribution of another layer to flow, since derivative plots are diagnostic plots that provide more meaning to dimensionless pressures. Fluid ratios are used in the field to pinpoint precisely which external boundary is causing flow. An growing gas-to-oil ratio would indicate that the gas cap is influencing flow, whereas an increasing water-to-oil ratio would indicate that the bottom water is influencing flow (23). In order to choose the optimum workovertechnique to reduce the production of undesired fluid, it is critical to identify the actual external contributions to flow fluid. In order to verify their findings,

Moreso, (23) computed dimensionless pressures and dimensionless pressure derivatives over a period of dimensionless time using two arbitrary values of dimensionless radius, rD = 1 and 10. The results obtained are depicted in Figs. 6a, 6b, and 7, which represent a vertical well producing oil from an infinite-acting reservoir. The pressure continued to rise monotonously over time, as seen in Fig.6. The pressure derivative in Fig. 2.8 grew monotonically and steadied at a value of 0.5 at the beginning of full radial flow, as can also be seen. Due to a wider sweep area than a dimensionless radius of 1, a wellbore with a dimensionless radius of 10 naturally takes longer to reach a derivative of 0.5.

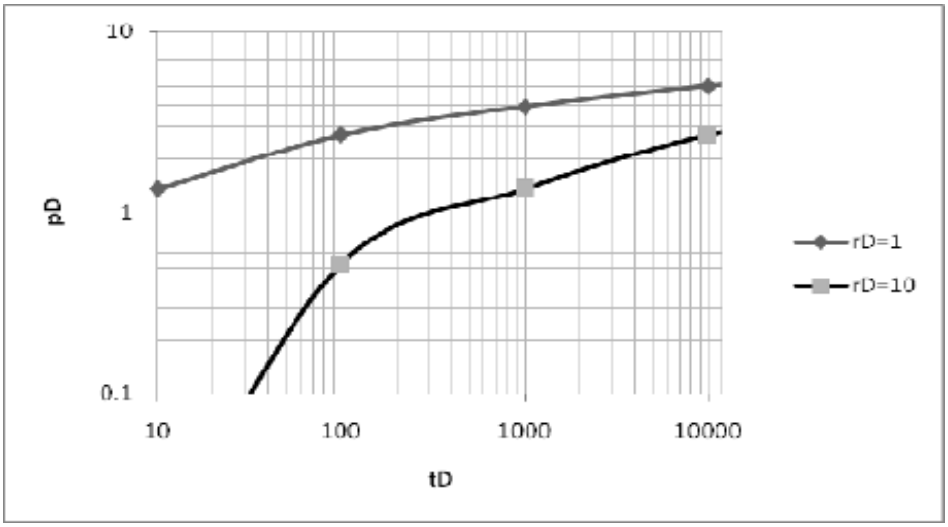

Fig.6a: Effects of layering on dimensionless pressure and pressure derivative for xD = 4.0 (23).

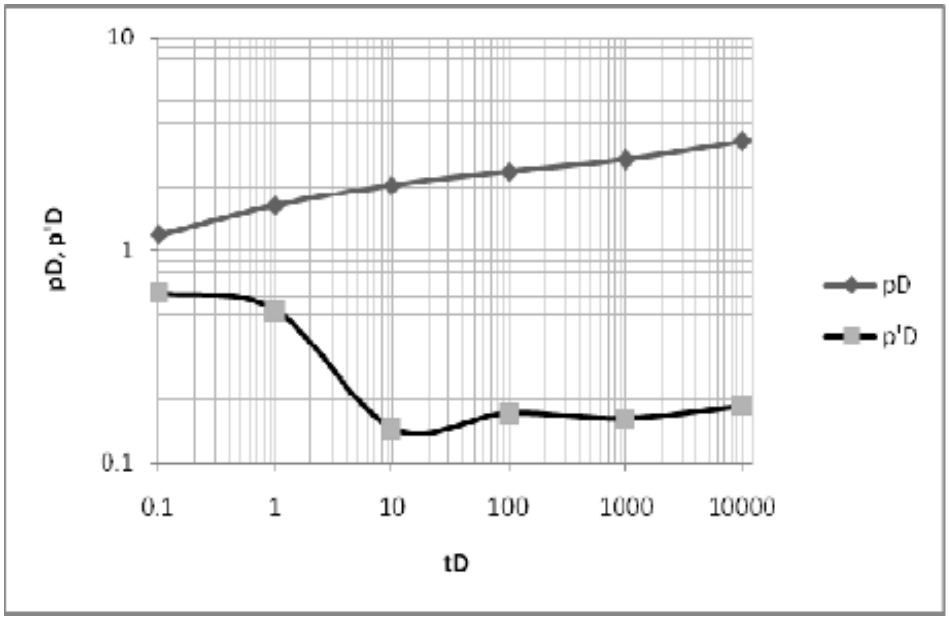

Fig. 6b: Dimensionless pressure for different radial positions (23).

ISSN 2278-2540 | DOI: 10.51583/IJLTEMAS | Volume XII, Issue IX, September 2023

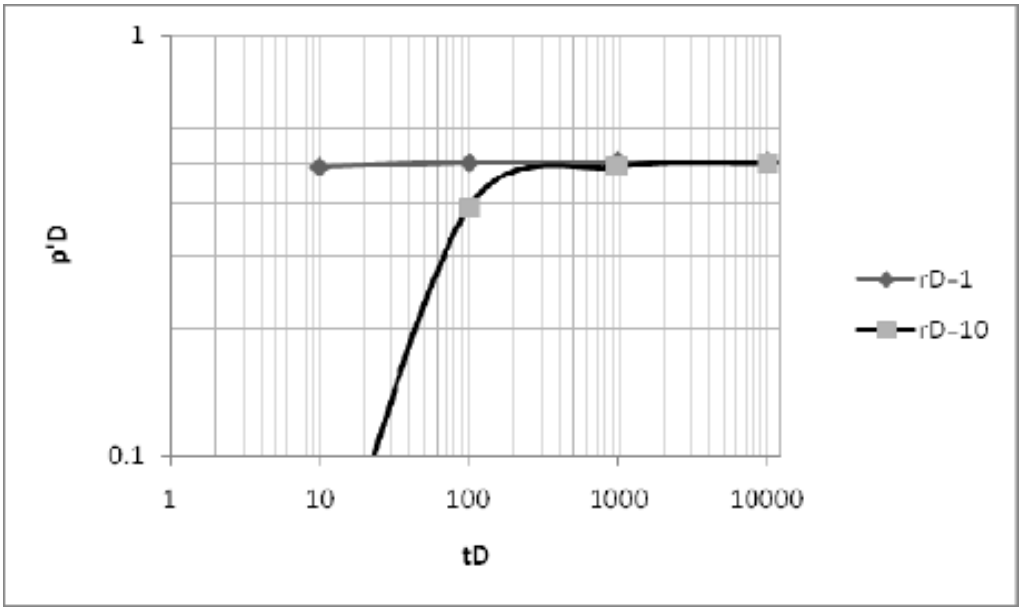

Fig.7: Dimension less pressure derivatives for different radial positions (23)

III. Methodology

This section give details information on use to achieve the goal of the study as shown in Fig. 9

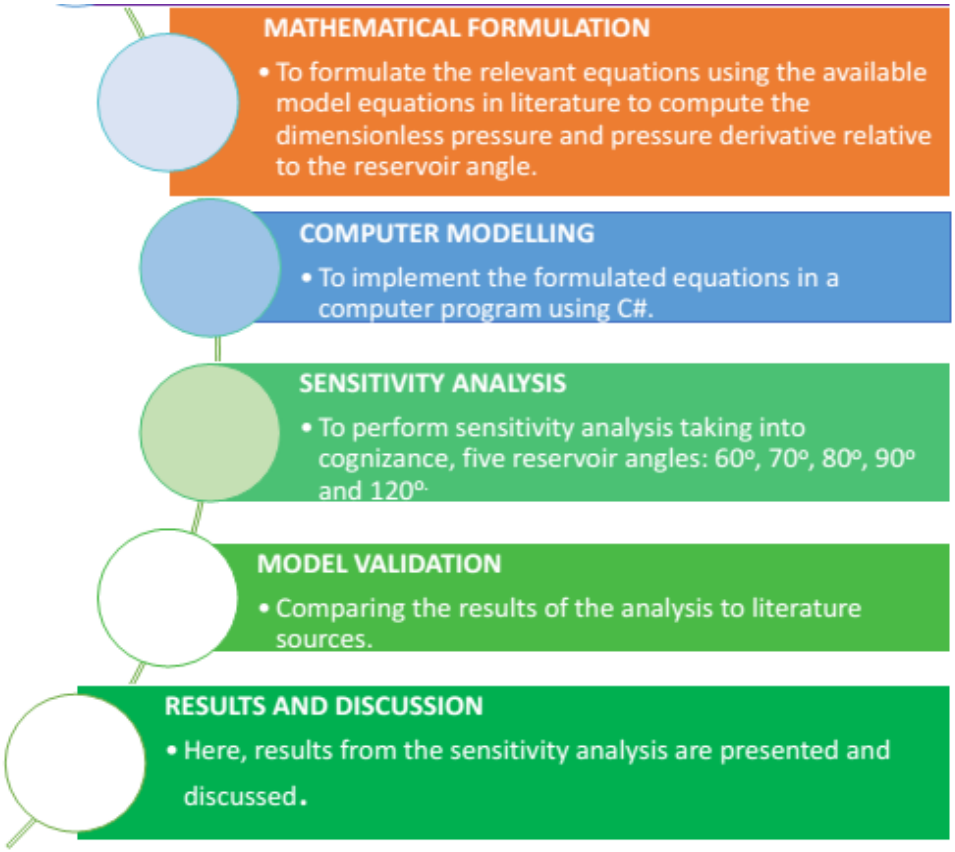

Fig. 8: Conceptual Framework of the study.

ISSN 2278-2540 | DOI: 10.51583/IJLTEMAS | Volume XII, Issue IX, September 2023

In Fig. 8, an overview of the research activities completed for this research is depicted. A vertical well was first thought to be confined by two inclined faults to define the problem to be solved. The dimensionless pressure and pressure derivative relative to the reservoir angle were computed using the model equations that were made accessible in the literature. Third, to put the formulated equations and mathematical models in this study effort into practice, a computer application was created utilizing the C# programming language. Fourth, a sensitivity analysis was carried out while considering five reservoir angles: 60°, 70°, 80°, 90°, and 120°. Then, for interpretation, the analysis's results are presented on a log-log scale graph. By contrasting the findings of this study with findings from other literary sources, the conclusions of this study were validated.

Problem description

Consider two sealing faults at an angle of (theta) to one another enclosing a vertical well with a radius of r_D=1.000 that was constructed independently. For the object well position, the pressure distribution is simulated with d = (0.500, 0.500), (0.550, 0.750), and (2.250, 0.815). This definition was employed in the simulation carried out in this investigation and was taken from (8). The reservoir angles that need to be taken into account are: 60°, 70°, 80°, 90°, and 120°. A basic sketch, as seen in Fig. 9, illustrates the geometry of the problem as it is explained

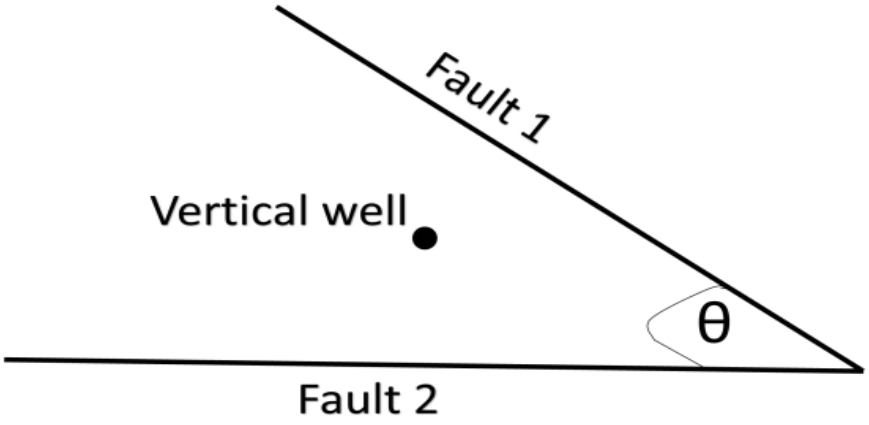

Fig. 9: A vertical well bounded by two sealing faults inclined at an angle Θ.

Mathematical Formulations

In this study, wells completed near a pair of sealing faults inclined at angle theta, to each other are considered, but the reservoir is infinite-acting in directions away from these faults. The reservoir is considered to be homogeneous and isotropic in nature, with a constant flow rate and negligible skin/wellbore storage effects. The early radial flow period only is taken into account for the derivation of mathematical formulation of the vertices.

(1) defined the dimensionless pressure drop of a vertical well using equations 8 to 10:

$$P_D = -\frac{1}{2} Ei\left(-\frac{r_D^2}{4t_D}\right) - - - - - - - - - \quad (8)$$

The pressure derivative of eq. 9 is expressed as follows:

$$P_D^2 = -\frac{1}{2} exp\left(-\frac{r_D^2}{4t_D}\right) - - - - - - - - \quad (9)$$

Where P_D= dimensionless pressure P_D^I = dimensionless pressure derivative

r_D= dimensionless radius

t_D= dimensionless time

$$Ei(x) = -\int_x^{\infty} \frac{e^{-u}}{u} du = lnx - \frac{x}{1!} + \frac{x^2}{2(2!)} - \frac{x^3}{3(3!)} + \cdots - - - - - - - - - - - - - - - - \quad (10)$$

ISSN 2278-2540 | DOI: 10.51583/IJLTEMAS | Volume XII, Issue IX, September 2023

But according to (24) the formula for calculating the quantity, N, of image wells that are produced when mirror-like sealing boundaries are angled θ toward one another is as shown in equation 10a, and 10b:

$$N\frac{360}{\theta}\left(if\frac{360}{\theta}isodd\right)----10a$$

$$N\frac{360}{\theta}-1\ \left(if\frac{360}{\theta}iseven\right)----10$$

The following mathematical formula in equations 11, and 12, however, show the dimensionless pressure and pressure derivative formulae for a vertical well bordered by two sealing defects.

$$P_D=-\frac{1}{2}\left[ln\frac{4t_D}{\gamma r_D^2}+\frac{4t_D}{\gamma r_1^2}+\frac{4t_D}{\gamma r_2^2}+\cdots+ln\frac{4t_D}{\gamma d_{N-1}^2}+ln\frac{4t_D}{\gamma d_N^2}\right]---11$$

$$P_D^1=\frac{N+1}{2t_D}+0.5\,ln\frac{4t_D}{\gamma r_D^2}+\sum_{i-1}^{N}0.5\ln\frac{4t_D}{\gamma d_i^2}-----12$$

Where $\gamma = Euler'sconstant$ = 1.781di=dimensionless distance of ith image well to object well Method

IV. Results and discussion

The following Figs. 10 to 21, and Table 1 displays the outcomes of using the developed program, OBLIQ:

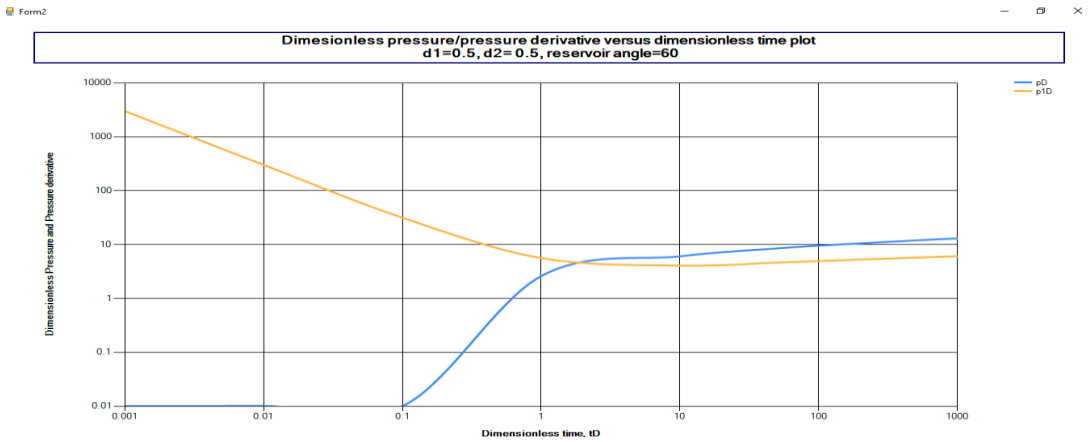

Fig. 10: Pressure derivative plot at angle 60° (d1=0.5, d2= 0.5)

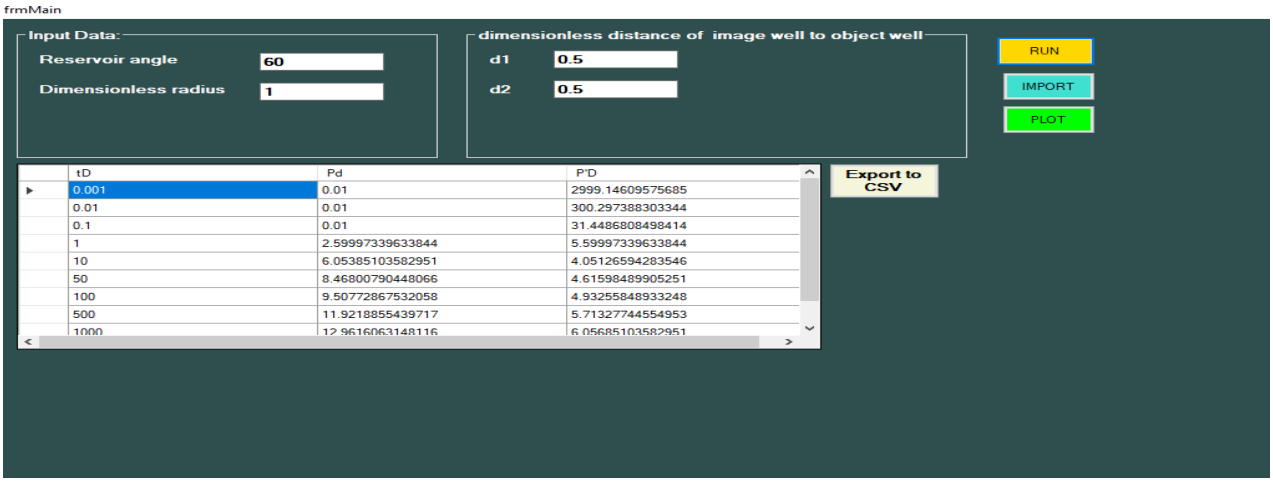

Fig. 11: Calculated variables at a reservoir angle of 60°

ISSN 2278-2540 | DOI: 10.51583/IJLTEMAS | Volume XII, Issue IX, September 2023

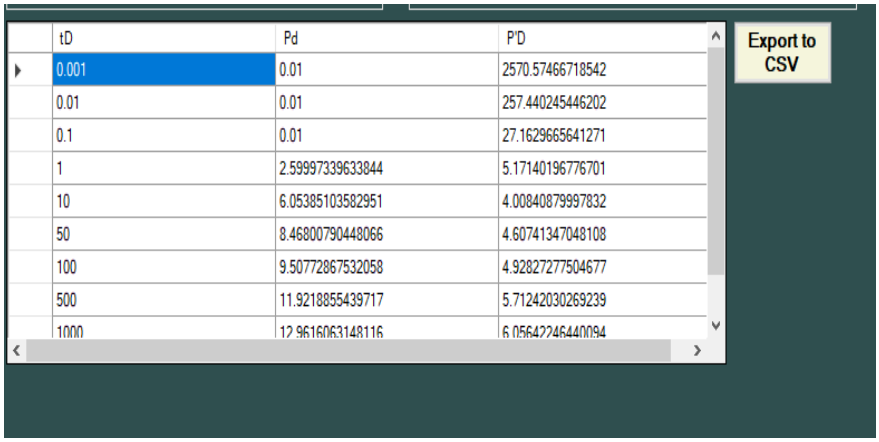

tD	Pd	P'D
0.001	0.01	2570.57466718542
0.01	0.01	257.440245446202
0.1	0.01	27.1629665641271
1	2.59997339633844	5.17140196776701
10	6.05385103582951	4.00840879997832
50	8.46800790448066	4.60741347048108
100	9.50772867532058	4.92827277504677
500	11.9218855439717	5.71242030269239
1000	12.9616063148116	6.05642246440094

Fig. 12: Calculated variables at reservoir angle of 70º (d1=0.5, d2= 0.5)

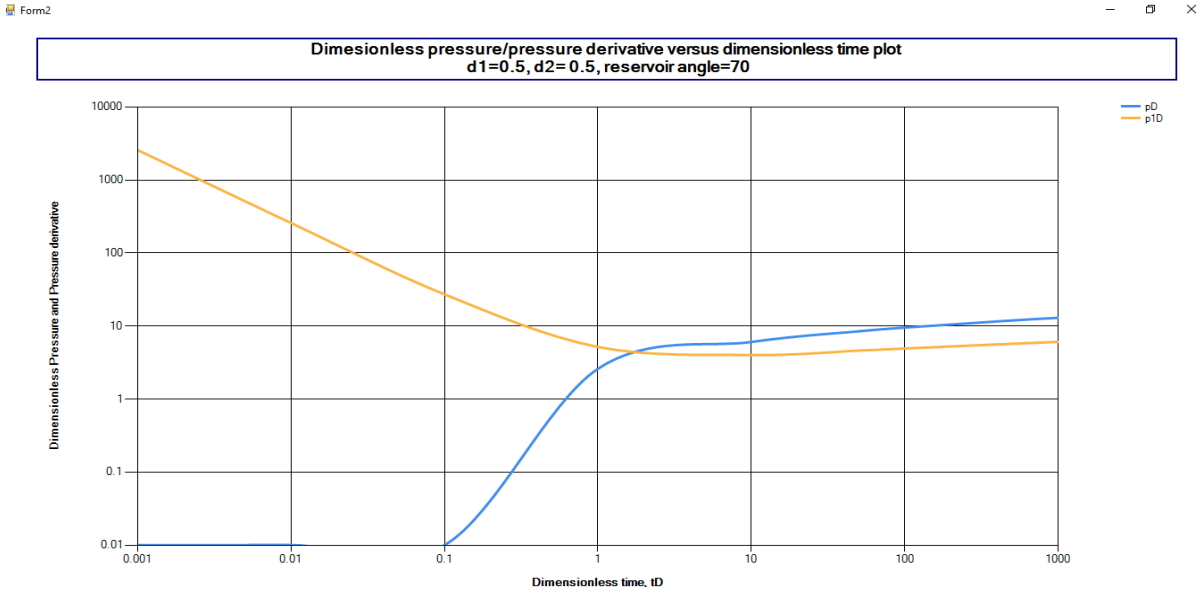

Fig. 13: Vertical well performance plot at 70º

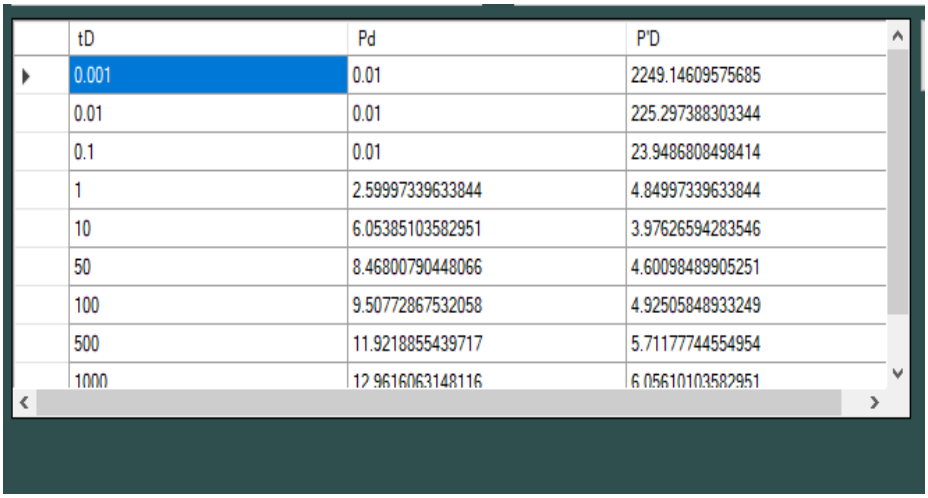

tD	Pd	P'D
0.001	0.01	2249.14609575685
0.01	0.01	225.297388303344
0.1	0.01	23.9486808498414
1	2.59997339633844	4.84997339633844
10	6.05385103582951	3.97626594283546
50	8.46800790448066	4.60098489905251
100	9.50772867532058	4.92505848933249
500	11.9218855439717	5.71177744554954
1000	12.9616063148116	6.05610103582951

Fig. 14: Calculated variables at reservoir angle of 80º (d1=0.5, d2= 0.5)

ISSN 2278-2540 | DOI: 10.51583/IJLTEMAS | Volume XII, Issue IX, September 2023

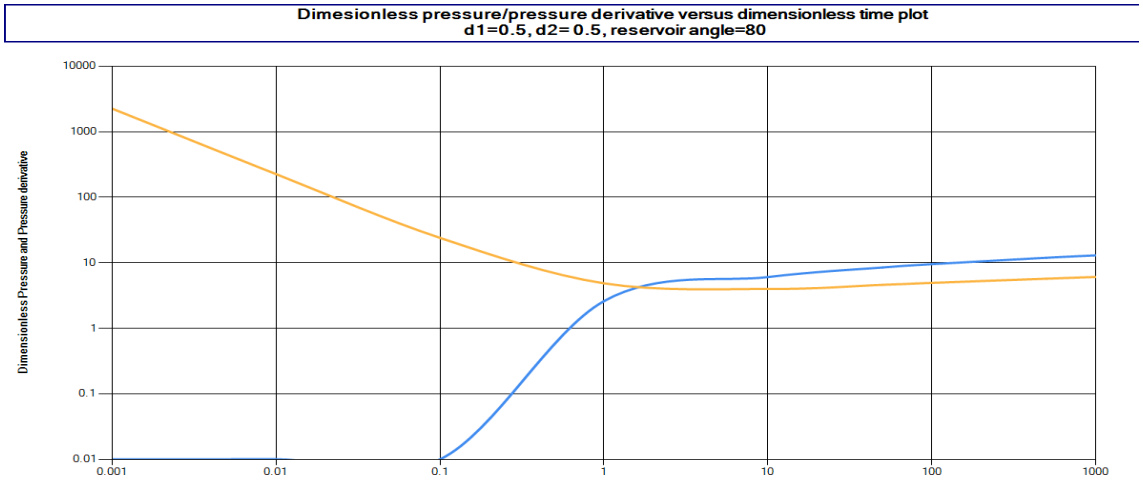

Fig. 15: Vertical well performance plot 80o

	tD	Pd	P'D
▶	0.001	0.01	1999.14609575685
	0.01	0.01	200.297388303344
	0.1	0.01	21.4486808498414
	1	2.59997339633844	4.59997339633844
	10	6.05385103582951	3.95126594283546
	50	8.46800790448066	4.59598489905251
	100	9.50772867532058	4.92255848933249
	500	11.9218855439717	5.71127744554954
	1000	12.9616063148116	6.05585103582951

Fig. 16: Calculated variables at reservoir angle of 90º (d1=0.5, d2= 0.5)

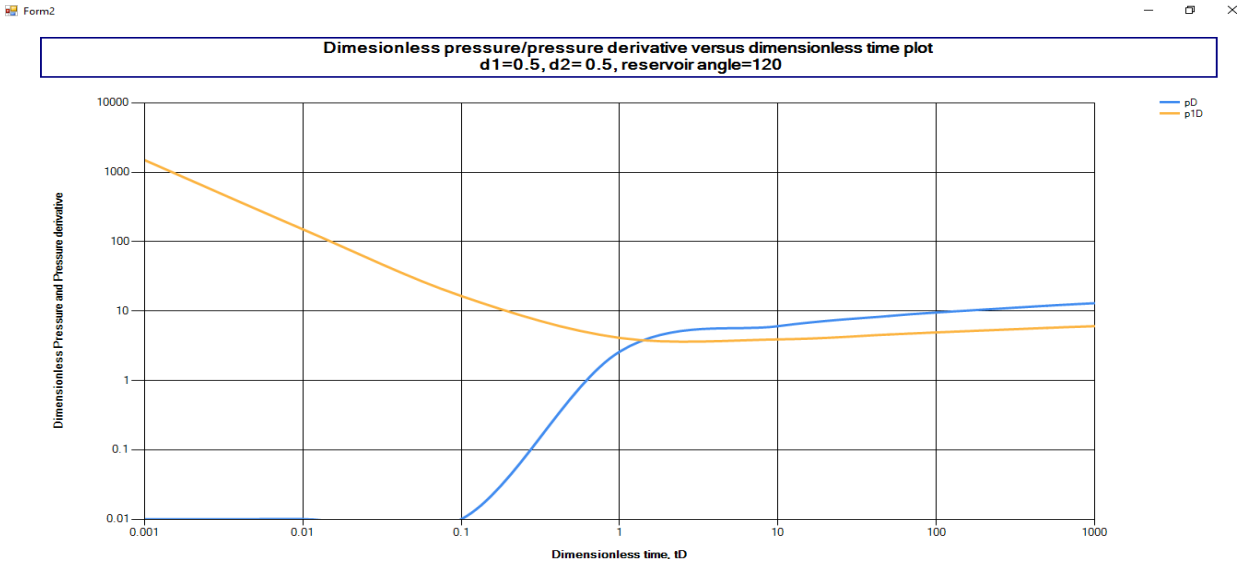

Fig. 17: Vertical well performance chart at angle 90º (d1=0.5, d2= 0.5)

ISSN 2278-2540 | DOI: 10.51583/IJLTEMAS | Volume XII, Issue IX, September 2023

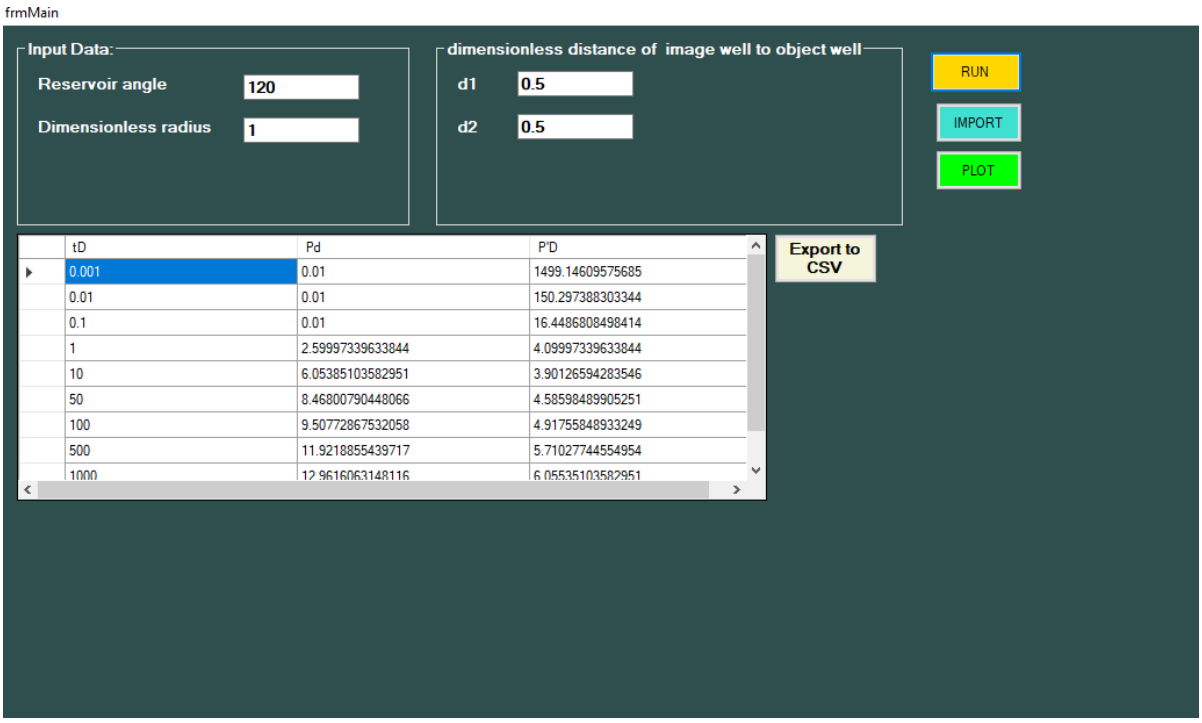

tD	Pd	P'D
0.001	0.01	1499.14609575685
0.01	0.01	150.297388303344
0.1	0.01	16.4486808498414
1	2.59997339633844	4.09997339633844
10	6.05385103582951	3.90126594283546
50	8.46800790448066	4.58598489905251
100	9.50772867532058	4.91755848933249
500	11.9218855439717	5.71027744554954
1000	12.9616063148116	6.05535103582951

Fig. 18: Calculated variables at reservoir angle of 120º (d1=0.5, d2= 0.5)

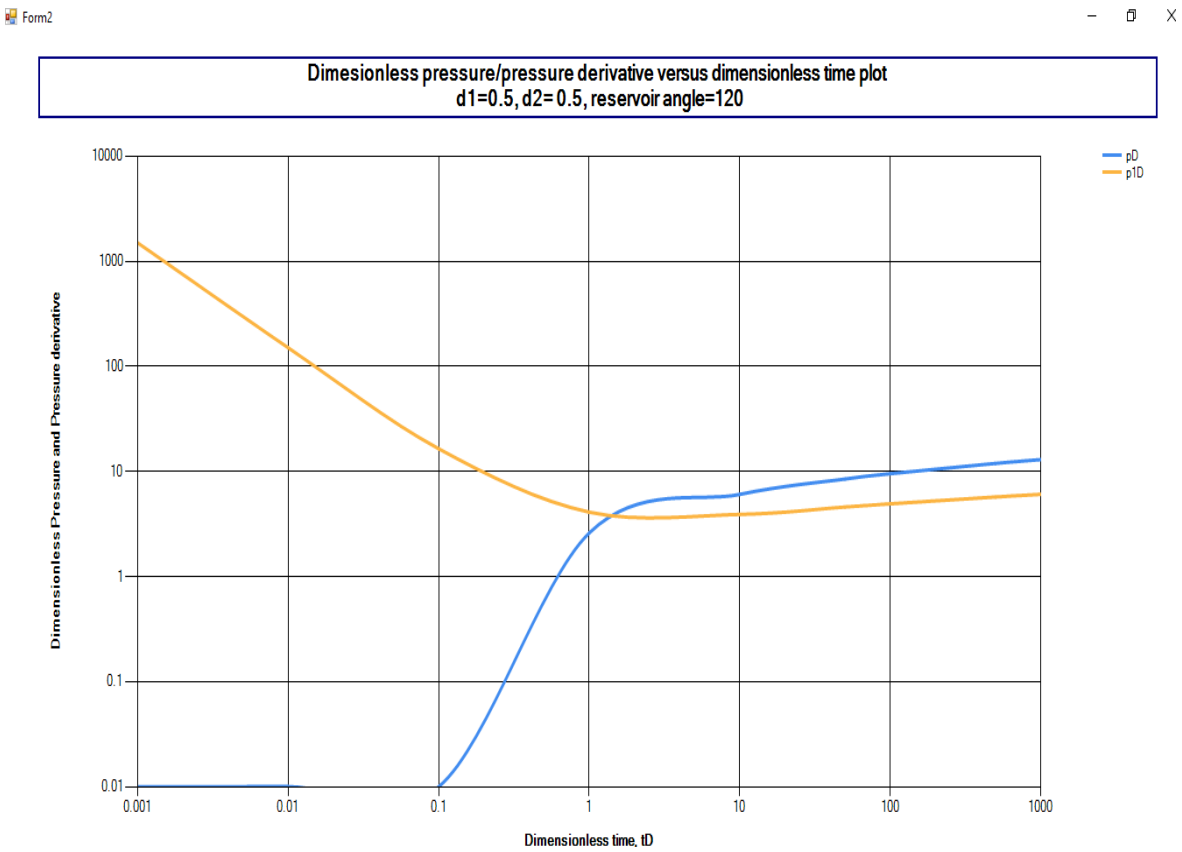

Fig. 19: Vertical well performance chart at angle 120º (d1=0.5, d2= 0.5)

ISSN 2278-2540 | DOI: 10.51583/IJLTEMAS | Volume XII, Issue IX, September 2023

Table 1: Reservoir angle and pressure derivatives relationship at t_D=0.001

Reservoirangle (degrees)	P^1D
60	2999.146
70	2570.49
80	2249.16
90	1999.15
120	1499.15

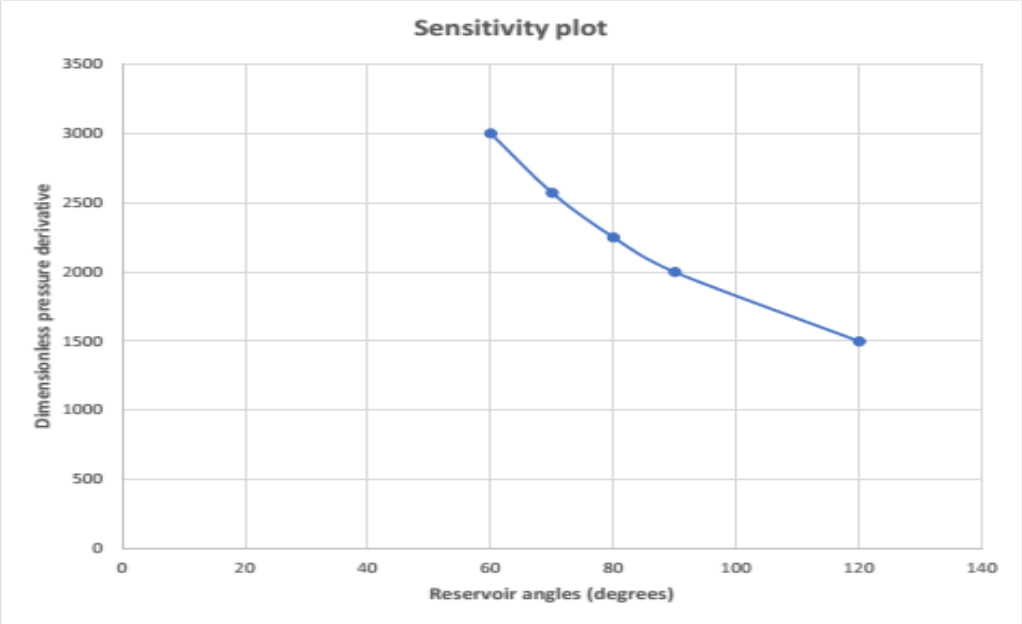

Fig. 20: Sensitivity plot showing the effect of reservoir angle on dimensionless pressure `derivative at t_D=0.001(d1=0.5, d2= 0.5)

V. Discussion

Discussion of results from varying the reservoir angles at a fixed dimensionless distance of image well from object wells (d1=0.5, d2=0.5). Several dimensionless time t_D, ranging from 0.001 to 10,000, as well as a fixed value of dimensionless radius (r_D) of 1 and at a reservoir angle of 60^o were employed as input parameters while using the developed toolkit (OBLIQ). A log-log chart of the outcome is displayed in Fig. 9. Dimensionless pressure, or PD, was seen to increase in the graph from 0.01 to 12.96. In the meantime, it was seen that the pressure derivative had hyperbolically decreased from 2999.15 to 1499.15. However, this decline reflects the fact that the dimensionless pressure has decreased. Lower reservoir angles result in decreasing derivatives. Fig. 12 shows the derived variables for the dimensionless pressure and pressure derivatives at a 60° angle. Similar to what was done above, the following reservoir angles were also repeated: 70°, 80°, 90°, and 120°. The dimensionless pressure (PD) grew gradually and consistently from 0.01 (at t_D=0.01) to 12.96 (at t_D=1000) at a reservoir angle of 70^o. The dimensionless pressure derivative, however, was calculated to be 2570.49 at tD=0.001 (see Figures 12, and 13). It was noted that the pressure derivative at 70^o dropped in comparison to the reservoir angle of 60^o at a t_D=0.001. This decrease in the pressure derivative at a reservoir angle of 70° demonstrates how sensitive P1D is to this angle. The dimensionless pressure (PD), on the other hand, was shown to remain constant despite changes in the reservoir angle, suggesting that the dimensionless pressure derivative of a vertical well is the only one affected by the reservoir angle. Additionally, it was noted that at both reservoir angles of 60° and 70°, the change in pressure derivative was negligible from a dimensionless time of 10 and above. Similar to this, the created OBLIQUE tool was used to simulate the vertical oil well performance with reservoir angles of 80°, 90°, and 120°. According to the simulation's findings, the dimensionless pressure derivative for 80° was 2249.16 at t_D=0.001, for 90° it was 1999.16 at t_D=0.001, and for 120° it was 1499.16 at tD=0.00 (see Figs. 14 and 15). The facts that increased reservoir angles cause a lower dimensionless pressure derivative are therefore further

ISSN 2278-2540 | DOI: 10.51583/IJLTEMAS | Volume XII, Issue IX, September 2023

supported. Reduced well performance is indicated by a drop in pressure derivative because the well will have less energy to push the crude from its pay zones to the wellbore. Therefore, the angle of inclination between the faults must be modest to ensure increased production from the vertical oil well, which is bordered by two sealing faults inclined at an angle. For each of the five reservoir angles used in this study, a sensitivity analysis was conducted at a fixed dimensionless duration of 0.001 and a fixed dimensionless radius of 1.0. The outcome demonstrates that the dimensionless pressure derivative increases with decreasing reservoir angle, improving vertical well performance (See Fig. 20 and Table 1).

Model Validation

To verify the conclusions drawn from the simulation run for this study. A related study project was sourced from different sources of literature. According to (8), the plot of dimensionless pressure and its derivative against dimensionless time, t_D, is shown in the trend of the chart in Fig. 21. At a reservoir angle of 90°, the chart's trend was calculated. contrasting the chart in Fig. 11 with the one in Fig. 16, which was created for this study. It can be inferred that the outcome of this investigation is compatible with previous research.

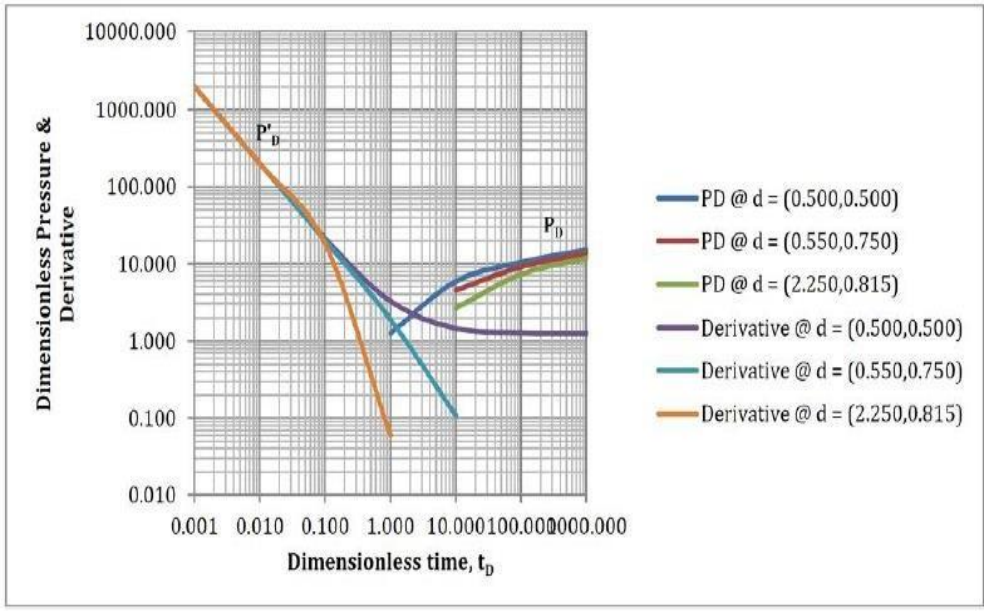

Fig. 21: Vertical oil well performance plot from a literary source (8)

VI. Conclusion and Recommendation

This study has shown how reservoir angle affects dimensionless pressure and derivatives of pressure. The aforementioned pressure variables contribute to the definition of oil well productivity. However, vertical oil wells were of particular interest in this study. In this study, empirical mathematical models for characterizing vertical oil wells bordered by two sealing faults were used. A reservoir supported by a robust aquifer was considered. To assess the impact of changing the reservoir angle on dimensionless pressure and pressure derivatives, the computer software OBLIQ was created. The mathematical models developed by (1) are applied by computer software. After consideration, it was found that lower reservoir angles produce greater values for pressure derivatives, which is indicative of a productive well. Simply said, high-pressure derivatives suggest that the aquifer is powerful enough to sweep oil from the reservoir's pore throat to the wellbore. To evaluate the impact of the reservoir angle on dimensionless pressure and pressure derivatives, a sensitivity analysis was also conducted utilizing a fixed value of dimensionless time to study various reservoir angle values. However, it was shown that the dimensionless pressure, PD, is unaffected by the reservoir angle. However, it was shown that the dimensionless pressure derivative (P') and the reservoir angles had an inverse connection. To validate the accuracy of the results, a comparison analysis was done between the results found in the literature and those found in the constructed computer model, OBLIQ. The analysis's findings demonstrated that the study's findings and those in the literature are consistent.

References

1. Matthews, C. S., & Russell, D. (1967). Pressure Buildu and Flow test in Wells. Society of Petroleum Engineers of AIME.

ISSN 2278-2540 | DOI: 10.51583/IJLTEMAS | Volume XII, Issue IX, September 2023

2. Jones, P. (1962) Reservoir Limit Test on Gas Wells. Journal of Petroleum Technology, 14, 613-619. https://doi.org/10.2118/24-PA
3. Prasad Raj K. (1975): Pressure Transient Analysis in the Presence Of Two Intersecting Boundaries. J Pet Technol 27 (01): 89–96. Paper Number: SPE- 4560-PA
4. Britto, P.R., Grader, A.S. (1988). The Effects of Size, Shape, and Orientation of an Impermeable Region on Transient Pressure Testing. One Petro. 3(3):595-606. https://doi.org/10.2118/16376-PA
5. Ogbamikhumi A. V and Adewole E. S. (2020): Pressure Behaviour Of A Horizontal Well Sandwiched Between Two Parallel Sealing Faults. Nigerian Journal of Technology (NIJOTECH). Vol. 39, No. 1, January 2020, pp. 148 – 153
6. Trabelsi, R.Boukadi, F.Seibi, A. Allen,D. Sebring, F.. Mannon, T Trabelsi H. (2017).Transient Pressure Behavior of a Well Located between a Constant Pressure Boundary and a Sealing Fault. **Natural Resources**, 8(10):
7. Ojah, M.,Onah, C., Adewole, S. E., Emumena, E. Onah, C.(2020). Determination of Optimal Well Location in Bounded Reservoirs Using the Dimensionless Pressure Derivative. Conference: SPE Nigeria Annual International Conference and Exhibition. DOI: 10.2118/203627-MS
8. Ogbamikhumi, A. V., &Adewole, E. S. (2021). Characteristics of Dimensionless Pressure Gradients and Derivatives of Horizontal and Vertical Wells Completed within Inclined Sealing Faults. Society of Petroleum Engineers
9. Horner, D.R. (1951) Pressure Build-Up in Wells. Proceedings of the 3rd World Petroleum Congress, 25-43.
10. Daley, T.M., Feighner, M.A., Majer, E.L., 2000. Monitoring underground gas storage in a fractured reservoir using time lapse VSP, Lawrence Berkeley National Laboratory Report LBNL-44876, Berkeley, CA, March, 129P
11. Boussila, A. K., Tiab, D. & Owayed, J. (2003). Pressure behavior of well near a leaky boundary in heterogeneous reservoirs. SPE Production and Operations Symposium, Oklahoma City, Oklahoma, USA. SPE 80911
12. Milkereit, B., Adam, E., Li, z., Qian, W., Bohlen, T., Banerjee, D., Schmitt, D.R., 2005. Multi-offset vertical seismic profiling: an experiment to assess petrophysical-scale parameters at the JAPEX/JNOC/GSC et al. Mallik 5L-38 gas hydrate production research well. in: Scientific results from the Mallik 2002 Gas Hydrate Production Research Well Program, Mackenzie Delta, Northwest Territories, Canada, edited by S. R. Dallimore and T. S. Collett, Bull. Geol. Surv. Can. 585, 13 pp.
13. Dowlath, J.,Onyeagoro, K.,Sookal, E., Quammie, K., Srinivasan, A. (2018). The Faults in our Fields – Well Count and Placement in a Columbus Basin Gas Field. Paper presented at the SPE Trinidad and Tobago Section Energy Resources Conference, Port of Spain, Trinidad and Tobago, June 2018.Paper Number: SPE-191226-MS https://doi.org/10.2118/191226-MS
14. Tiab, D. (1995). Analysis of pressure and pressure derivative without type-curve matching - skin and wellbore storage. J. Pet. Scie. Eng., 12(3), 171-181.
15. Stewart, R.R., Huddleston, P.D., Tze Kong, K., 1984. Seismic versus sonic velocities: A vertical seismic profiling study. Geophysics, 49: 1153-1168.
16. Bixel, H. C., Larkin, B. K. & van Poolen, H. K. (1963). Effect of linear discontinuities on pressure buildup and drawdown behavior. J. Pet. Technol., 15(8), 885-895
17. Abdelaziz, B., Tiab, D. (2004) Pressure Behaviour of a Well Between Two Intersecting Leaky Faults. DOI: 10.2118/2004-209.
18. Yaxley L. M. (1987) Effect of a Partially Communicating Fault on Transient Pressure Behavior SPE Form Eval 2 (04): 590–598.Paper Number: SPE-14311-PAhttps://doi.org/10.2118/14311-PA.
19. Eiroboy, I., Wilkie, S. I. (2017). Comparative Evaluation of Pressure Distribution Between Horizontal And Vertical Wells In A Reservoir (Edge Water Drive). Nigerian Journal of Technology, 457-460.
20. Tarek, A., & Paul, D. M. (2005). Advanced Reservoir Engineering. Elsevier.
21. Gringarten, A. C., & Ramey, H. J. (1973). The Use of Source and Green's Functions in Solving Unsteady-Flow Problems in Reservoirs. Society of Petroleum Engineering Journal , 285– 296.
22. Edobhiye, O., &Adewole, E. S. (2014). Effects of Both Wellbore and Reservoir Properties on Dimensionless Pressure and Dimensionless Pressure Derivative Distribution of a Horizontal Well in a Reservoir Subject to Bottom Water i, Gas Cap and Single Edge Water Drive Mechanisms. Society of Petroleum Engineers, 1-10.
23. Owolabi, A. F., Olafuyi, O. A., &Adewole, E. S. (2012). Pressure distribution in a layered Reservoir with gas-cap and bottom water. . Nigeria journal Technology, 189-198.
24. James J. Butler Jr. and Ming-shuTsou 1(2003): Pumping-induced leakage in a bounded aquifer: An example of a scale-invariant phenomenon Water Resources Research, Vol. 39, No. 12, 1344, doi:10.1029/2002WR001484, 200